Histomorphology of the subregions of the scapholunate ligament and its enthesis

Journal of Wrist Surgery

Histomorphology of the subregions of the scapholunate ligament and its enthesis

--Manuscript Draft--

Manuscript Number:	JWS-D-20-00044R1
Full Title:	Histomorphology of the subregions of the scapholunate ligament and its enthesis
Short Title:	Scapholunate ligament histomorphology
Article Type:	Basic Science Research Article
Keywords:	scapholunate; ligament; enthesis; morphology; histology
Corresponding Author:	Philippa A Rust, MBBS, MD, FRCS(Tr & Orth), DipHandSurg The Hooper Hand Unit Livingston, UNITED KINGDOM
Corresponding Author Secondary Information:	
Corresponding Author's Institution:	The Hooper Hand Unit
Corresponding Author's Secondary Institution:	
First Author:	Mei Yen Liew, Third year medical student
First Author Secondary Information:	
Order of Authors:	Mei Yen Liew, Third year medical student
	Jeremy W Mortimer, BMedSci(Hons), MSc, BMBS, MRCS(Eng)
	Jennifer Z Paxton, BSc (Hons), MSc, PhD
	Stephen Tham, MBBS
	Philippa A Rust, MBBS, MD, FRCS(Tr & Orth), DipHandSurg
Order of Authors Secondary Information:	
Abstract:	Background The scapholunate interosseous ligament (SLIL) has three subregions- dorsal, proximal and volar. The SLIL enthesis has not previously been studied despite its important mechanical function in wrist joint biomechanics. Questions/Purposes This study aims to compare the histomorphological differences between the SLIL subregions, including at their entheses. Three questions are explored: Do the gross dimensions differ between SLIL subregions? Does the enthesis qualitatively, and its calcified fibrocartilage (CF) quantitatively, differ between (a) SLIL subregions and (b) scaphoid and lunate attachments? Methods Twelve fresh-frozen human cadaveric wrists were dissected and the gross dimensions of the SLIL subregions measured. Subregions were histologically processed for morphological and compositional analyses, including quantification of enthesis CF area. Results The dorsal subregion was the thickest. The dorsal and volar subregions had fibrocartilaginous entheses while the proximal subregion was attached to articular cartilage. The dorsal subregion had significantly more CF than the volar subregion. There was no significant difference in the enthesis CF between scaphoid and lunate

	attachments in the three subregions. Conclusions There are significant morphological differences between the SLIL subregions. The dorsal subregion has the largest amount of CF, which is consistent with the greater biomechanical force subjected to this subregion. The similar histomorphology of the ligament at the scaphoid and lunate entheses suggests that similar biomechanical forces are applied to both attachments. Clinical relevance The histomorphological results confirm that the dorsal subregion is the strongest of the three subregions. The results from the entheseal region may have important implications in the study of graft incorporation during SLIL reconstruction.
Response to Reviewers:	Dear Editor, Thank you for your comments. We have made the necessary changes and attached updated files.
Additional Information:	
Question	**Response**
Please state number of references in your manuscript	31
Total number of words	2611
Total number of videos	0
Total number of B/W figures	2
Total number of tables	0
Total number of colour figures	6

Letter of submission of Manuscript

Dear Editors,

We are submitting a manuscript entitled 'Histomorphology of the subregions of the scapholunate interosseous ligament and its enthesis' for publication in *The Journal of Wrist Surgery.*

This is for special section on the scapholunate ligament.
Attn Stephen Tham

With the submission of this manuscript I would like to assure the following:

This manuscript has not under consideration for publishing elsewhere, accepted for publication elsewhere, or under editorial review for publication elsewhere.

All authors have been actively involved in the planning and enactment of the study and have also assisted with the preparation of the submitted article. All the authors have approved the contents of this manuscript and have agreed to the Journal of Wrist Surgery's submission policies.

The references have been checked and are correct.

The authors have read the Journal's Instructions to Authors and the paper conforms to these instructions in all respects.

With this letter, I am submitting the following documents:

- Title page
- Manuscript, including abstract and main text
- References
- Figures
- Ethical review signed statement
- Conflict of interest statements

Thank you for your kind consideration.

Yours sincerely,

Mei Yen Liew
First Author

Philippa A Rust
Corresponding Author

April 2020

TITLE PAGE

A) Title:

Histomorphology of the subregions of the scapholunate interosseous ligament and its enthesis

B) Running title:

Scapholunate ligament histomorphology

C) Author details:

1) Name: Mei Yen Liew

Final degree: third year medical student at the University of Edinburgh Medical School

Title: Miss

Department: Hooper Hand Unit, Department Plastic Surgery

Affiliation: Anatomy, Edinburgh Medical School: Biomedical Sciences, University of Edinburgh, Scotland, UK.

Address: Hooper Hand Unit, St John's Hospital, Howden Road West, Livingston, EH54 6PP

E-mail address: s1705439@sms.ed.ac.uk

2) Name: Jeremy W. Mortimer

Final degrees: BMedSci(Hons), MSc, BMBS, MRCS(Eng)

Title: Mr

Department: Anatomy, Edinburgh Medical School: Biomedical Sciences

Affiliation: University of Edinburgh, Scotland, UK.

Address: Old Medical School, Teviot Place, Edinburgh, EH8 9AG

E-mail address: j.w.mortimer@sms.ed.ac.uk

3) Name: Jennifer Z. Paxton

Final degrees: BSc (Hons), MSc, PhD

Title: Dr

Department: Anatomy, Edinburgh Medical School: Biomedical Sciences

Affiliation: University of Edinburgh, Scotland, UK.

Address: Old Medical School, Teviot Place, Edinburgh, EH8 9AG

E-mail address: j.z.paxton@ed.ac.uk

4) Name: Stephen Tham

Final degrees: MBBS

Title: Mr

Department: Plastic and Hand Surgery, St Vincents Hospital, Melbourne, Australia

Affiliation: Hand and Wrist Biomechanics Laboratory/O'Brien Institute, Melbourne, Australia

Address: 41 Victoria Parade, Fitzroy Victoria 3065, Australia

E-mail address: stham@bigpond.net.au

5) Name: Philippa A. Rust

Final degrees: MBBS, MD, FRCS(Tr & Orth), DipHandSurg, MFSTEd

Title: Miss

Department: Hooper Hand Unit, Department Plastic Surgery

Affiliation: Anatomy, Edinburgh Medical School: Biomedical Sciences, University of Edinburgh, Scotland, UK.

Address: Hooper Hand Unit, St John's Hospital, Howden Road West, Livingston, EH54 6PP

E-mail address: philippa.rust@ed.ac.uk

D) Conflict of interest statement:

The authors disclose receipt of the following financial support for the research, authorship, and/or publication of this article: This research received grants from Hand and Wrist Medical Research Foundation, a charitable body registered in Melbourne, Australia and grants from TBC: Mr Hamilton's Research and Development Fund, St John's Hospital, Edinburgh, during the conduct of the study.

E) Ethical review committee statement:

No ethical review process was required for undertaking this study. All specimens used in this study were obtained from Anatomy, The University of Edinburgh in accordance with the Human Tissue (Scotland) Act 2006.

F) Statement of the location where the work was performed (only if authors from multiple institutions):

This work was performed at the University of Edinburgh, Scotland, UK.

G) Word count: 2611 words

H) Corresponding Author:

Name: Philippa A. Rust

E-mail address: philippa.rust@ed.ac.uk

Mailing address: Hooper Hand Unit, St John's Hospital, Howden Road West, Livingston, EH54 6PP

Telephone number: +44 (0)1506 523118

Acknowledgements

We thank the body donors and their families who made this study possible. We also thank Iain Campbell for his crucial assistance in the anatomy teaching laboratory. We thank Christina Loukopoulou for her much-valued presence during gross measurements of SLIL subregions and her guidance in editing dissection images. We also thank Yousef Abdulaziz Almajed and Abdulaziz Alomiery for their input in CF quantification methods.

Abstract

Background

The scapholunate interosseous ligament (SLIL) has three subregions- dorsal, proximal and volar. The SLIL enthesis has not previously been studied despite its important mechanical function in wrist joint biomechanics.

Questions/Purposes

This study aims to compare the histomorphological differences between the SLIL subregions, including at their entheses. Three questions are explored: Do the gross dimensions differ between SLIL subregions? Does the enthesis qualitatively, and its calcified fibrocartilage (CF) quantitatively, differ between (a) SLIL subregions and (b) scaphoid and lunate attachments?

Methods

Twelve fresh-frozen human cadaveric wrists were dissected and the gross dimensions of the SLIL subregions measured. Subregions were histologically processed for morphological and compositional analyses, including quantification of enthesis CF area.

Results

The dorsal subregion was the thickest. The dorsal and volar subregions had fibrocartilaginous entheses while the proximal subregion was attached to articular cartilage. The dorsal subregion had significantly more CF than the volar subregion. There was no significant difference in the enthesis CF between scaphoid and lunate attachments in the three subregions.

Conclusions

There are significant morphological differences between the SLIL subregions. The dorsal subregion has the largest amount of CF, which is consistent with the greater biomechanical force subjected to this subregion. The similar histomorphology of the ligament

at the scaphoid and lunate entheses suggests that similar biomechanical forces are applied to both attachments.

Clinical relevance

The histomorphological results confirm that the dorsal subregion is the strongest of the three subregions. The results from the entheseal region may have important implications in the study of graft incorporation during SLIL reconstruction.

Keywords: scapholunate, ligament, enthesis, morphology, histology

Introduction

The scapholunate interosseous ligament (SLIL) has a unique C-shape[1] which was historically considered as a single ligament consisting of two portions[2]. More recent studies have since defined the SLIL as a single unit with three subregions: dorsal, proximal and volar[1-3]. The SLIL is the primary stabilizer of the scapholunate articulation[4,5]. SLIL injury follows a progression of ligamentous tearing from the volar to the dorsal subregion[6]. The ligament typically avulses from the scaphoid and remains attached to the lunate in acute injuries[5,7,8]. If left untreated, this ligament usually does not spontaneously heal and the position of the carpus changes resulting in a predictable pattern of arthritis[5,9]. The current most common surgical reconstruction technique is a modified Brunelli procedure[10]. The aim of this procedure is to restore carpal alignment by using part of a flexor carpi radialis tendon graft passed from volar to dorsal through a tunnel in the scaphoid and attachingit to the dorsal aspect of the lunate[10]. More recently, and without long-term surgical follow-up results, bone-ligament-bone graft procedures have been described[9,11] and these typically focused on reconstructing the dorsal subregion due to ease of surgical access[12]. Evidence suggests that the dorsal is the strongest and most important subregion to maintain scapholunate interval stability[5,13,14]. However, a review of the current literature show reports varying on the biomechanical strength between different subregions[3].

The enthesis is a specialized region where a tendon, ligament or joint capsule attaches to bone allowing smooth transition of force between soft tissue and bone[15]. Entheses are classified as either fibrous or fibrocartilaginous according to the type of tissue found at the attachment site[15,16]. A fibrocartilaginous enthesis is characterized by four zones of tissue: dense fibrous connective tissue, uncalcified fibrocartilage (UF), calcified fibrocartilage (CF) and bone[15,17]. There is a tidemark between the UF and CF zones which acts as the mechanical boundary between soft and hard tissues[18]. This attachment site has been widely studied in

other anatomical areas such as the anterior cruciate ligament of the knee[17,19] but it has not previously been studied in the SLIL.

The quantification of enthesis CF provides information about load and maximum force transmitted through the ligament-bone junction[15-17,20]. Previous biomechanical studies were not uniform on the tensile strength of different SLIL subregions[3,12,21,22]. Histological quantification of CF area may help to elucidate biomechanical functionality between subregions, as functional adaptation of tissue structure to mechanical force adheres to the 'form follows function' principle which underpins Wolff's law[20,23]. The gross and histological anatomy of the SLIL have been described in previous studies[1,3,13,24-26]. However, a systematic review by Buijze et al.[2] reported inconsistencies in the sub-regional SLIL description.

This study aims to compare sub-regional macroscopic and microscopic morphology, including at their entheses, to resolve discrepancies in previously reported studies and better understand the prioritization of any subregion in reconstruction after SLIL injury. A further aim is to compare the entheses of both the scaphoid and lunate to establish differences which may inform the relative frequency of injury between the two bones and to better understand how graft material, used for ligament reconstruction, needs to be incorporated in the bone-ligament interface. The questions explored are: Do the gross dimensions differ between the SLIL subregions? Does the enthesis qualitatively, and its calcified fibrocartilage (CF) quantitatively, differ between (a) SLIL subregions and (b) scaphoid and lunate?

Materials and Methods

Study Design

A total of twelve wrists from ten fresh-frozen cadavers (age range 61 – 87 years; mean 75.8 years; six males, four females) were dissected. All specimens were donated to the University of Edinburgh Medical School body donation programme, under the regulations of

the Human Tissue (Scotland) Act 2006. The twelve dissected wrists were made up of a left and right wrist from two cadaveric donors and either the left or right wrist from the remaining eight donors. Upon dissection, the SLIL of three wrists showed signs of degeneration and detachment from the carpal bones and were excluded from the study. The remaining nine wrists (all from different cadaveric donors) were taken forward for further analysis.

All wrists specimens were dissected through a longitudinal skin incision, with a standard dorsal approach to expose the scaphoid and lunate bones with the intervening SLIL (Figure 1). A section through the scaphoid and through the lunate bones with the SLIL intact between them was removed (Figure 2). Once samples were dissected, they were immediately fixed in 10% neutral buffered formalin (Sigma-Aldrich, USA) at 4°C for 48 hours.

The samples were next decalcified in 'Decalcifying Solution-Lite' (Sigma-Aldrich, USA), for 14 to 72 hours, dependant on the size of specimen. The samples were then dehydrated through a series of ethanol concentrations using a VIP E300 tissue processor (Sakura Tissue-Tek, Japan) and mounted in paraffin wax blocks. 10μm sections were cut using a Leica RM 2245 microtome (Leica Microsystems Ltd, UK) parallel with the ligament length, including both bone insertions, at approximately 50% through each SLIL subregion (Figure 3). Multiple sections were mounted onto glass slides and stained with 0.1% toluidine blue (Sigma-Aldrich, USA). The stained slides were scanned using a NanoZoomer-XR C12000 digital slide scanner (Hamamatsu Photonics, Japan) to obtain high resolution images of the sections for analysis of the SLIL entheses.

Outcome Measures

On first exposure of the SLIL in dissection, the gross measurements of each SLIL subregion were taken using a digital Vernier calliper, capable of registering to 0.01mm accuracy. Three dimensions were measured: ligament thickness, width and length (Figure 3).

For qualitative and quantitative histological study, scanned images of stained sections were analyzed using ImageJ image analysis software (National Institute of Health, USA). Three sections per subregion per wrist were analyzed, and quantitative measurements averaged per subregion. The tissue composition of the ligaments and entheses were observed. In addition, the enthesis profile, defined as the shape of the tidemark at the ligament-bone junction, was categorized as either straight, concave, convex, mixed (concave+convex) or complex (multiple concave+convex profiles). Four quantitative measurements were determined, adapted from a method by Beaulieu et al[17] - linear enthesis length, segmented enthesis length, CF cross-sectional area, and CF relative area. The linear enthesis length was defined as the linear distance between the edges of the enthesis at the hard-soft tissue junction (enthesis tidemark) (Figures 4A, 4B and 4C). The segmented enthesis length measurement accounted for the curvature of the enthesis by plotting nine points at equidistant intervals (12.5% increments) along the entire linear length and then extrapolating the points perpendicularly to the upper edge of the tidemark (Figure 4D). The enthesis distance was then measured from start to finish between these segmented points.

The CF cross-sectional area was defined by the area between the tidemark and the CF-cortical bone junction (Figure 4D). In entheses with multiple tidemarks, the tidemark furthest from the CF-cortical bone junction was selected. The CF relative area was calculated by dividing the CF cross-sectional area by the segmented enthesis length. This method was different from that utilised by Beaulieu et al.[17], which divided the CF area by linear enthesis length, in order to control for the curvature of the SLIL entheses. The segmented length was chosen as it was more representative of the curved enthesis profile.

Statistical Analysis

Statistical tests were carried out using SPSS Version 24.0 (IBM Corporation, USA) on confirmed normally-distributed data using the Shapiro-Wilk normality test. Repeated

measures ANOVA with a Bonferroni post-hoc analysis was used to compare the gross dimension measurements for each SLIL subregion. Paired t-tests were used to compare the CF area between dorsal and volar SLIL subregions for each bone. Similarly, paired t-tests were used to compare between scaphoid and lunate attachment for each subregion. Statistical significance was defined as $p < 0.05$.

Results

From the gross measurements taken (Figure 3), the SLIL dorsal subregion was significantly thicker than the other subregions (Figure 5). There were no other significant differences between subregions within other dimensions measured.

From our histological study, the overall composition of the SLIL was different between the three subregions. The dorsal and volar subregions were made up of fibrous connective tissue but the fibrous tissue density was much higher in the dorsal subregion (Figure 6A). The volar subregion had more loosely connected fibrous tissue (Figure 6C). The proximal subregion consisted mainly of fibrocartilage connective tissue (Figure 6B). The dorsal and volar subregions at both the scaphoid and lunate attachments were fibrocartilaginous entheses whereas the proximal subregion inserted into cortical bone via articular cartilage (Figure 7). The tidemark of the enthesis was continuous across the adjacent articular cartilage at either end of the enthesis in the dorsal and volar subregions. Both the dorsal and proximal subregions had a mostly convex enthesis profile (Dorsal- 50% convex, 27.8% mixed and 22.2% straight; Proximal- 81.3% convex, 12.5% mixed and 6.2% straight). 62.5% of the volar subregion had a complex enthesis profile, 25% were mixed, the rest equally distributed between straight and convex. None of the subregions had a solely concave enthesis profile.

From the measure of enthesis CF, the dorsal subregion had significantly more CF than the volar subregion. The dorsal subregion was 1.97 times thicker than the volar subregion

(value calculated by comparing mean CF relative area between the two subregions at both scaphoid and lunate attachments). There were no significant differences in enthesis CF area between the scaphoid and lunate in either subregion (Figure 8). Analysis of the linear and segmented enthesis lengths showed no significant differences between the subregions or between the scaphoid and lunate.

Discussion

The enthesis is the region where a tendon, ligament or joint capsule attaches to bone[15]. It has been widely studied in other anatomical areas such as the anterior cruciate ligament of the knee[17,19], but there is no existing literature on the enthesis of the SLIL. This ligament is divided into three subregions: dorsal, proximal and volar[1]. Surgical reconstruction following SLIL injury commonly employs a modification of the Brunelli technique, recreating the scapholunate positioning, with the tendon graft passing through the scaphoid, out dorsally and attaching onto the lunate in the dorsal subregion[13]. When bone-ligament-bone grafts are used, the graft is placed through a more accessible dorsal wrist arthrotomy[7,12]. Previous evidence suggested that this is the strongest and most important subregion to maintain scapholunate interval stability[3,27]. However, a recent review reported inconsistencies in the biomechanical strength and functionality between different SLIL subregions[3].

This study acknowledges a number of limitations. Sample size was limited and within a regional population. Differences described were however clear and seen in comparison of all wrist specimens, suggesting a population trait. The age range of cadaveric specimens was between 61 to 87 years old. The enthesis is known to undergo age-related degeneration, including an increase in thickness of CF[17,28], however this seems very unlikely to potentially affect one bone or subregion preferentially[17]. We would postulate that the comparative differences found will still be present in a younger population. Analysis of the SLIL, a three-dimensional structure, was performed using two-dimensional images. Every effort was made

to achieve reliable and consistent region sampling of sections at the middle 50% of each subregion, in a plane perpendicular to the articular surface of the carpal bones (Figure 3).

The thickness measurement was the main gross morphological difference between the SLIL subregions. Our results showed that the dorsal subregion was on average twice as thick as the proximal or volar subregion. A systematic review by Buijze et al.[2] highlighted controversies on gross measurements of SLIL subregions. These authors reported average gross measurements based on their review of four different studies[1,25,26,29]. Our results on ligament thickness and length mirrored the overall measurements reported in this systematic review[2]. This verifies that the dorsal subregion is indeed much thicker than the other two subregions while there is no significant difference in ligament length between subregions. However, there were discrepancies between our width measurements and the measurements previously reported. Our review of those studies revealed that the authors did not specify their technique of ligament measurements. This, coupled with the difficulty in measuring a 'linear' width for a 'curved' C-shaped SLIL, could be possible explanations for these discrepancies.

The dorsal and volar subregions were mainly collagenous while the proximal subregion was largely fibrocartilaginous, in agreement with findings from previous studies[1,24]. Hence, it is natural to postulate a fundamental difference between the proximal and dorsal/volar subregions in terms of function due to their different principal tissue types. This is consistent with the clinical finding of perforations seen solely in the proximal SLIL subregion at wrist arthroscopy, not causing scapholunate instability. From our results, the entheses at the dorsal and volar subregions could be classified as fibrocartilaginous entheses with four zones of tissue found at the attachment site: dense fibrous connective tissue, UF, CF and cortical bone. The fibrocartilage in the proximal subregion inserted into cortical bone via articular cartilage and the four distinct tissue zones were not present. This finding

suggests a key difference in biomechanical functionality between the proximal and the dorsal and volar subregions as the quantity of each tissue type found is characteristic of mechanical loading at the enthesis[17,20].

The quantification of fibrocartilaginous enthesis CF informs about load and maximum force transmitting through the attachment site[17,19,20,30]. We considered relative quantitative enthesis comparison between the dorsal and volar subregions possible as they had fibrocartilaginous entheses, while the proximal subregion did not and was thus excluded. Previous biomechanical studies focused mainly on the dorsal subregion[3]. The few biomechanical studies which conducted comparisons between the three subregions found varying results[3]: most agreed that the dorsal subregion was the strongest[5,7,11,12,24,26], Nikolopoulos et al.[21] reported approximately equal strength between the dorsal and volar subregions, while Logan et al.[22] reported that the volar subregion was the strongest. However, the general consensus was that the proximal subregion is the only subregion which is not considered in SLIL reconstruction due to its smallest mechanical contribution[3,12,24]. A greater CF area is a measure of greater mechanical force at the enthesis[18,30,31]. Our study showed that the dorsal subregion had a much greater CF area compared to the volar subregion. This suggests that the dorsal subregion takes the greatest load and therefore is the most important subregion in supporting the scapholunate interval. This is supported by previous biomechanical studies which agreed that the dorsal subregion is subjected to the greatest biomechanical force[5,7,11,12,24,26]. Since the relative CF area, which controlled for different insertion lengths of the enthesis, showed a similar doubling of CF area in the dorsal compared to volar subregion, the dorsal CF area could also be described as twice as thick, further emphasizing the greater load transmitted through this subregion. Clinical studies have shown that avulsion tends to occur from the scaphoid attachment in acute injuries[5,7,8]. Our study found no significant difference in CF area between the scaphoid and lunate in all three

subregions. This suggests that other factors, including pattern of force transfer during injury, may have more influence on SLIL avulsion sites.

In conclusion, there are significant differences in macroscopic and microscopic morphology between the SLIL subregions. Our results, coupled with analysis of previous literature, confirms that we should consider the SLIL as three distinct morphological subregions, for reconstruction and function[6]. We found the dorsal subregion to be the thickest and contain the greatest proportion of CF, consistent with its role as the most important SLIL subregion for biomechanical strength and to maintain scapholunate interval stability. However, we found no significant difference in proportion of CF between the scaphoid and lunate attachments of the ligament, suggesting that this is not the main factor in determining the site of ligament avulsion. Further studies can be carried out to examine other factors influencing ligament avulsion from either carpal bone in acute injuries. This study also provides insight into the bone-ligament interface and tissue ingrowth necessary for the successful incorporation of neoligament graft material.

References

1. Berger RA. The gross and histologic anatomy of the scapholunate interosseous ligament. J Hand Surg Am. 1996;21(2):170-178

2. Buijze GA, Lozano-Calderon SA, Strackee SD, Blankevoort L, Jupiter JB. Osseous and ligamentous scaphoid anatomy: Part I. A systematic literature review highlighting controversies. J Hand Surg Am. 2011;36(12):1926-1935

3. Rajan PV, Day CS. Scapholunate interosseous ligament anatomy and biomechanics. J Hand Surg Am. 2015;40(8):1692-1702

4. Chim H, Moran SL. Wrist essentials: the diagnosis and management of scapholunate ligament injuries. Plast Reconstr Surg. 2014;134(2):312e-322e

5. Mullikin I, Srinivasan RC, Bagg M. Current techniques in scapholunate ligament reconstruction. Orthop Clin North Am. 2020;51(1):77-86

6. Mayfield JK, Johnson RP, Kilcoyne RK. Carpal dislocations: pathomechanics and progressive perilunar instability. J Hand Surg Am. 1980;5(3):226-241

7. Kitay A, Wolfe SW. Scapholunate instability: current concepts in diagnosis and management. J Hand Surg Am. 2012;37(10):2175-2196

8. Andersson JK, Garcia-Elias M. Dorsal scapholunate ligament injury: a classification of clinical forms. J Hand Surg Eur Vol. 2013;38(2):165-169

9. White NJ, Rollick NC. Injuries of the scapholunate interosseous ligament: an update. J Am Acad Orthop Surg. 2015;23(11):691-703

10. Garcia-Elias M, Lluch AL, Stanley JK. Three-ligament tenodesis for the treatment of scapholunate dissociation: indications and surgical technique. J Hand Surg Am. 2006;31(1):125-134

11. Walsh JJ, Berger RA, Cooney WP. Current status of scapholunate interosseous ligament injuries. J Am Acad Orthop Surg. 2002;10(1):32-42

12. Berger RA, Imeada T, Berglund L, An KN. Constraint and material properties of the subregions of the scapholunate interosseous ligament. J Hand Surg Am. 1999;24(5):953-962

13. Manske MC, Huang JI. The quantitative anatomy of the dorsal scapholunate interosseous ligament. Hand (N Y). 2019;14(1):80-85

14. Patterson RM, Yazaki N, Andersen CR, Viegas SF. Prediction of ligament length and carpal diastasis during wrist flexion-extension and after simulated scapholunate instability. J Hand Surg Am. 2013;38(3):509-518

15. Benjamin M, Kumai T, Milz S, Boszczyk BM, Boszczyk AA, Ralphs JR. The skeletal attachment of tendons--tendon "entheses". Comp Biochem Physiol A Mol Integr Physiol. 2002;133(4):931-945

16. Benjamin M, Ralphs JR. Fibrocartilage in tendons and ligaments--an adaptation to compressive load. J Anat. 1998;193 (Pt 4):481-494

17. Beaulieu ML, Carey GE, Schlecht SH, Wojtys EM, Ashton-Miller JA. Quantitative comparison of the microscopic anatomy of the human ACL femoral and tibial entheses. J Orthop Res. 2015;33(12):1811-1817

18. Apostolakos J, Durant TJ, Dwyer CR, et al. The enthesis: a review of the tendon-to-bone insertion. Muscles Ligaments Tendons J. 2014;4(3):333-342

19. Sasaki N, Ishibashi Y, Tsuda E, et al. The femoral insertion of the anterior cruciate ligament: discrepancy between macroscopic and histological observations. Arthroscopy. 2012;28(8):1135-1146

20. Benjamin M, Toumi H, Ralphs JR, Bydder G, Best TM, Milz S. Where tendons and ligaments meet bone: attachment sites ('entheses') in relation to exercise and/or mechanical load. J Anat. 2006;208(4):471-49021

21. Nikolopoulos FV, Apergis EP, Poulilios AD, Papagelopoulos PJ, Zoubos AV, Kefalas VA. Biomechanical properties of the scapholunate ligament and the importance of its portions in the capitate intrusion injury. Clin Biomech (Bristol, Avon). 2011;26(8):819-823

22. Logan SE, Nowak MD, Gould PL, Weeks PM. Biomechanical behavior of the scapholunate ligament. Biomed Sci Instrum. 1986;22:81-85

23. Milz S, Benjamin M, Putz R. Molecular parameters indicating adaptation to mechanical stress in fibrous connective tissue. Adv Anat Embryol Cell Biol. 2005;178:1-71

24. Mataliotakis G, Doukas M, Kostas I, Lykissas M, Batistatou A, Beris A. Sensory innervation of the subregions of the scapholunate interosseous ligament in relation to their structural composition. J Hand Surg Am. 2009;34(8):1413-1421

25. Nagao S, Patterson RM, Buford WL, Jr., Andersen CR, Shah MA, Viegas SF. Three-dimensional description of ligamentous attachments around the lunate. J Hand Surg Am. 2005;30(4):685-692

26. Sokolow C, Saffar P. Anatomy and histology of the scapholunate ligament. Hand Clin. 2001;17(1):77-81

27. Upal MA, Crisco JJ, Moore DC, Sonenblum SE, Wolfe SW. In vivo elongation of the palmar and dorsal scapholunate interosseous ligament. J Hand Surg Am. 2006;31(8):1326-1332

28. Villotte S, Knüsel CJ. Understanding entheseal changes: definition and life course changes. International Journal of Osteoarchaeology. 2013;23(2):135-146

29. Berger RA. The ligaments of the wrist. A current overview of anatomy with considerations of their potential functions. Hand Clin. 1997;13(1):63-82

30. Evans EJ, Benjamin M, Pemberton DJ. Variations in the amount of calcified tissue at the attachments of the quadriceps tendon and patellar ligament in man. J Anat. 1991;174:145-151

31. Benjamin M, Ralphs JR. Entheses--the bony attachments of tendons and ligaments. Ital J Anat Embryol. 2001;106(2 Suppl 1):151-157

Legends

Figure 1: Dissection of scaphoid and lunate bones with SLIL. Right wrist in hyperflexion.

Figure 2: Dissection of different subregions of the SLIL. Right wrist in hyperflexion. A) Using an 8mm osteotome and hammer, the scaphoid and lunate bones were sectioned approximately 8mm from the SLIL attachment to the bones. B) Arrow showing remaining scaphoid and lunate with proximal subregion of SLIL (pSLIL) in situ after the dorsal subregion was removed.

Figure 3: Dimensions of gross measurements taken at each SLIL subregion in a right wrist. Green arrows representing direction of sectioning using the microtome. ⊗ represents articulation with lunate bone. ⊙ represents articulation with scaphoid bone. T – thickness, W – width, L – length.

Figure 4: Quantification of calcified fibrocartilage cross-sectional area and enthesis length. All images are from the same section. A) Figure showing the SLIL attachment to the lunate and scaphoid bones. Enthesis straight length (black line) with arrow on the right marking the beginning of the enthesis while arrow on the left marking the furthest end of the enthesis, at the tidemark (purple line). B) Magnified image of A, with line and arrow showing the beginning of the enthesis at the scaphoid attachment. C) Magnified image of A, with line and arrow demarcating the transition between the end of the calcified fibrocartilage above and articular cartilage below at the scaphoid attachment. D) Magnified image of A at the scaphoid attachment, showing an e~~E~~xample of calcified fibrocartilage cross-sectional area (area enclosed by purple and red lines), ~~and~~ linear (black line) and segmented (yellow line) enthesis lengths. The calcified fibrocartilage cross-sectional area lies between the tidemark (purple line) and the calcified cartilage-cortical bone junction (red line). The segmented length is formed by extrapolating the short green lines on the linear enthesis length (black

line) to the tidemark. F – dense fibrous connective tissue, UF – uncalcified fibrocartilage, CF – calcified fibrocartilage, CB – cortical bone.

Figure 5: Differences between the gross measurements of SLIL subregions. Mean values with error bars indicating ± one standard error of mean. ** = $p < 0.01$.

Figure 6: SLIL subregions from the same wrist specimen stained with toluidine blue. A) Fibrous connective tissue of the dorsal subregion. B) Proximal subregion showing distinct purple staining of cartilage proteoglycans and presence of chondrocytes in the ligament region. C) Fibrous connective tissue of the volar subregion. dSLIL – dorsal SLIL, pSLIL – proximal SLIL, vSLIL – volar SLIL.

Figure 7: Magnified scaphoid enthesis of each SLIL subregion (from Figure 6). Arrows indicate enthesis tidemark. A) Dorsal subregion. B) Proximal subregion. C) Volar subregion. F – fibrous connective tissue, UF – uncalcified fibrocartilage, CF – calcified fibrocartilage, CB – cortical bone, L – ligament, AC – articular cartilage.

Figure 8: Quantification of CF area. A) Mean cross-sectional area of enthesis CF. B) Mean relative area of enthesis CF. Relative area was calculated by dividing CF cross-sectional area by the segmented enthesis length. Error bars indicating ± one standard error of mean. * = $p < 0.05$ and ** = $p < 0.01$.

Ethical Review Committee Statement

Manuscripts involving humans or human data must be accompanied by a copy of the letter from your ethical committee approving your study.

Alternatively, if no ethical committee approval was needed please complete and sign the form below and submit with your manuscript

Manuscript title:

Histomorphology of the subregions of the scapholunate interosseous ligament and its enthesis

---

Corresponding author:

Philippa A. Rust

As corresponding author I confirm that no ethical committee approval is needed for this manuscript

Signed: Philippa A. Rust

Date: 30.04.2020

References

1. Berger RA. The gross and histologic anatomy of the scapholunate interosseous ligament. J Hand Surg Am. 1996;21(2):170-178

2. Buijze GA, Lozano-Calderon SA, Strackee SD, Blankevoort L, Jupiter JB. Osseous and ligamentous scaphoid anatomy: Part I. A systematic literature review highlighting controversies. J Hand Surg Am. 2011;36(12):1926-1935

3. Rajan PV, Day CS. Scapholunate interosseous ligament anatomy and biomechanics. J Hand Surg Am. 2015;40(8):1692-1702

4. Chim H, Moran SL. Wrist essentials: the diagnosis and management of scapholunate ligament injuries. Plast Reconstr Surg. 2014;134(2):312e-322e

5. Mullikin I, Srinivasan RC, Bagg M. Current techniques in scapholunate ligament reconstruction. Orthop Clin North Am. 2020;51(1):77-86

6. Mayfield JK, Johnson RP, Kilcoyne RK. Carpal dislocations: pathomechanics and progressive perilunar instability. J Hand Surg Am. 1980;5(3):226-241

7. Kitay A, Wolfe SW. Scapholunate instability: current concepts in diagnosis and management. J Hand Surg Am. 2012;37(10):2175-2196

8. Andersson JK, Garcia-Elias M. Dorsal scapholunate ligament injury: a classification of clinical forms. J Hand Surg Eur Vol. 2013;38(2):165-169

9. White NJ, Rollick NC. Injuries of the scapholunate interosseous ligament: an update. J Am Acad Orthop Surg. 2015;23(11):691-703

10. Garcia-Elias M, Lluch AL, Stanley JK. Three-ligament tenodesis for the treatment of scapholunate dissociation: indications and surgical technique. J Hand Surg Am. 2006;31(1):125-134

11. Walsh JJ, Berger RA, Cooney WP. Current status of scapholunate interosseous ligament injuries. J Am Acad Orthop Surg. 2002;10(1):32-42

12. Berger RA, Imeada T, Berglund L, An KN. Constraint and material properties of the subregions of the scapholunate interosseous ligament. J Hand Surg Am. 1999;24(5):953-962

13. Manske MC, Huang JI. The quantitative anatomy of the dorsal scapholunate interosseous ligament. Hand (N Y). 2019;14(1):80-85

14. Patterson RM, Yazaki N, Andersen CR, Viegas SF. Prediction of ligament length and carpal diastasis during wrist flexion-extension and after simulated scapholunate instability. J Hand Surg Am. 2013;38(3):509-518

15. Benjamin M, Kumai T, Milz S, Boszczyk BM, Boszczyk AA, Ralphs JR. The skeletal attachment of tendons--tendon "entheses". Comp Biochem Physiol A Mol Integr Physiol. 2002;133(4):931-945

16. Benjamin M, Ralphs JR. Fibrocartilage in tendons and ligaments--an adaptation to compressive load. J Anat. 1998;193 (Pt 4):481-494

17. Beaulieu ML, Carey GE, Schlecht SH, Wojtys EM, Ashton-Miller JA. Quantitative comparison of the microscopic anatomy of the human ACL femoral and tibial entheses. J Orthop Res. 2015;33(12):1811-1817

18. Apostolakos J, Durant TJ, Dwyer CR, et al. The enthesis: a review of the tendon-to-bone insertion. Muscles Ligaments Tendons J. 2014;4(3):333-342

19. Sasaki N, Ishibashi Y, Tsuda E, et al. The femoral insertion of the anterior cruciate ligament: discrepancy between macroscopic and histological observations. Arthroscopy. 2012;28(8):1135-1146

20. Benjamin M, Toumi H, Ralphs JR, Bydder G, Best TM, Milz S. Where tendons and ligaments meet bone: attachment sites ('entheses') in relation to exercise and/or mechanical load. J Anat. 2006;208(4):471-49021

21. Nikolopoulos FV, Apergis EP, Poulilios AD, Papagelopoulos PJ, Zoubos AV, Kefalas VA. Biomechanical properties of the scapholunate ligament and the importance of its portions in the capitate intrusion injury. Clin Biomech (Bristol, Avon). 2011;26(8):819-823

22. Logan SE, Nowak MD, Gould PL, Weeks PM. Biomechanical behavior of the scapholunate ligament. Biomed Sci Instrum. 1986;22:81-85

23. Milz S, Benjamin M, Putz R. Molecular parameters indicating adaptation to mechanical stress in fibrous connective tissue. Adv Anat Embryol Cell Biol. 2005;178:1-71

24. Mataliotakis G, Doukas M, Kostas I, Lykissas M, Batistatou A, Beris A. Sensory innervation of the subregions of the scapholunate interosseous ligament in relation to their structural composition. J Hand Surg Am. 2009;34(8):1413-1421

25. Nagao S, Patterson RM, Buford WL, Jr., Andersen CR, Shah MA, Viegas SF. Three-dimensional description of ligamentous attachments around the lunate. J Hand Surg Am. 2005;30(4):685-692

26. Sokolow C, Saffar P. Anatomy and histology of the scapholunate ligament. Hand Clin. 2001;17(1):77-81

27. Upal MA, Crisco JJ, Moore DC, Sonenblum SE, Wolfe SW. In vivo elongation of the palmar and dorsal scapholunate interosseous ligament. J Hand Surg Am. 2006;31(8):1326-1332

28. Villotte S, Knüsel CJ. Understanding entheseal changes: definition and life course changes. International Journal of Osteoarchaeology. 2013;23(2):135-146

29. Berger RA. The ligaments of the wrist. A current overview of anatomy with considerations of their potential functions. Hand Clin. 1997;13(1):63-82

30. Evans EJ, Benjamin M, Pemberton DJ. Variations in the amount of calcified tissue at the attachments of the quadriceps tendon and patellar ligament in man. J Anat. 1991;174:145-151

31. Benjamin M, Ralphs JR. Entheses--the bony attachments of tendons and ligaments. Ital J Anat Embryol. 2001;106(2 Suppl 1):151-157

Figure 1

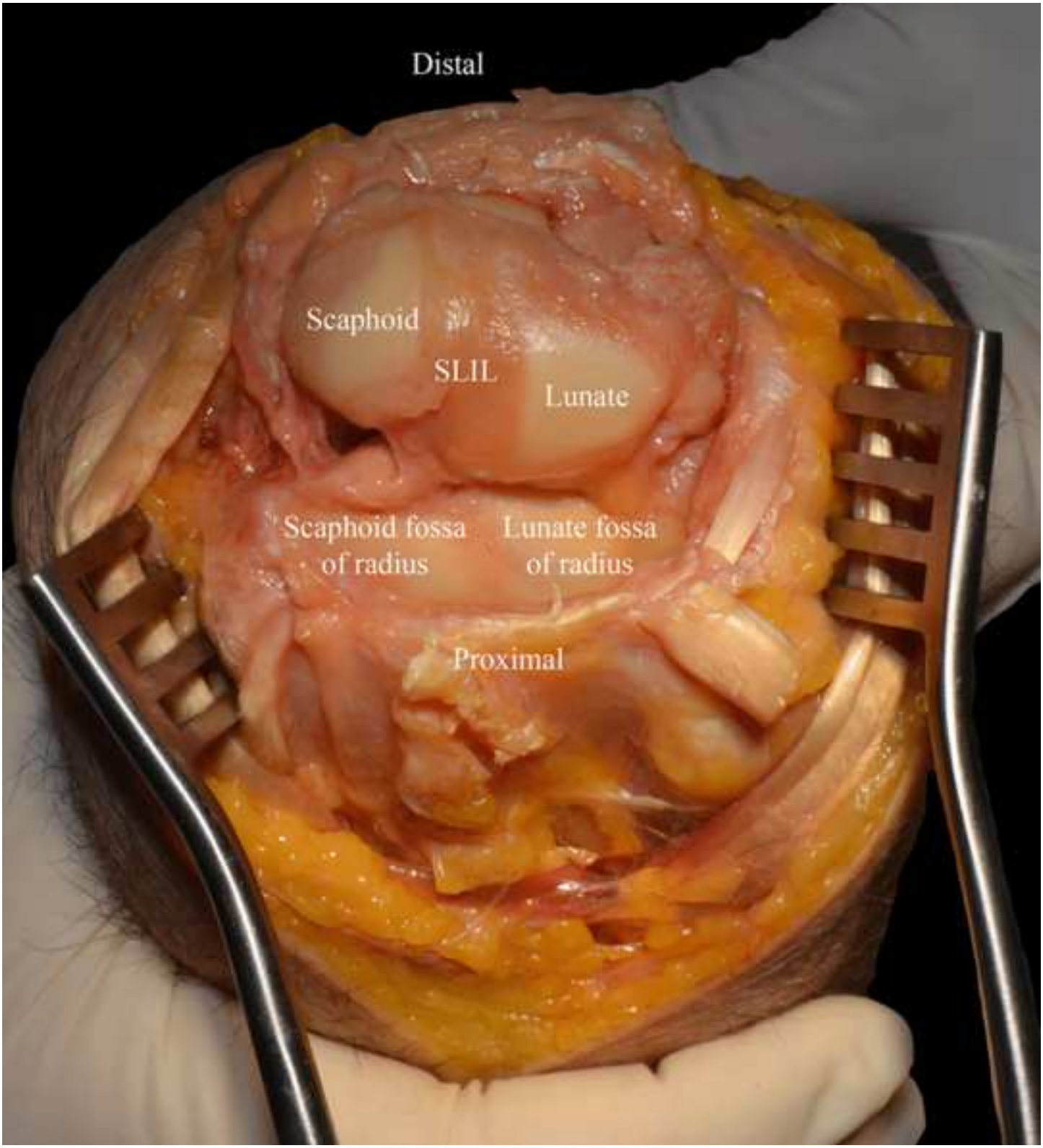

Figure 2

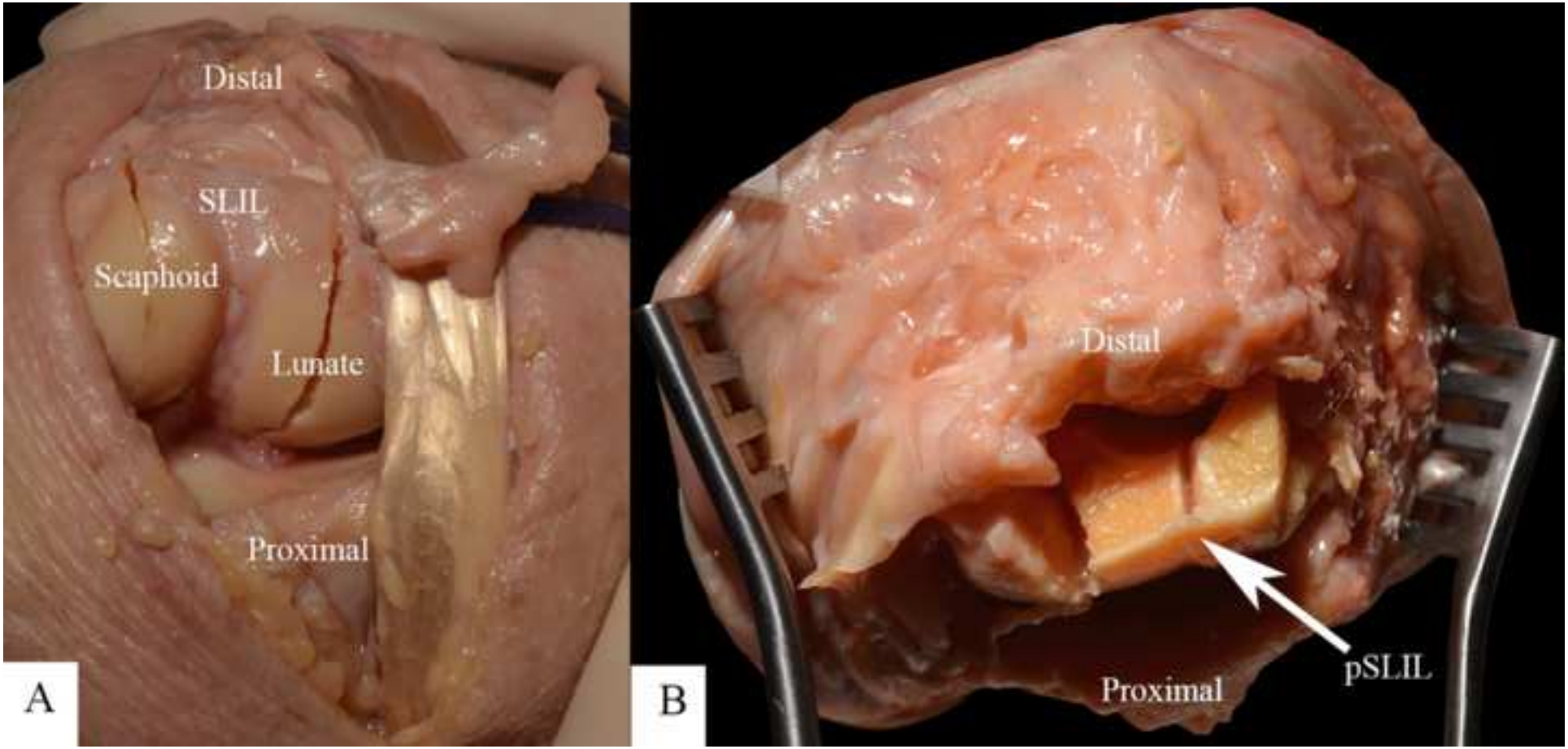

Figure 3

Click here to access/download;Figure;Figure 3.tif

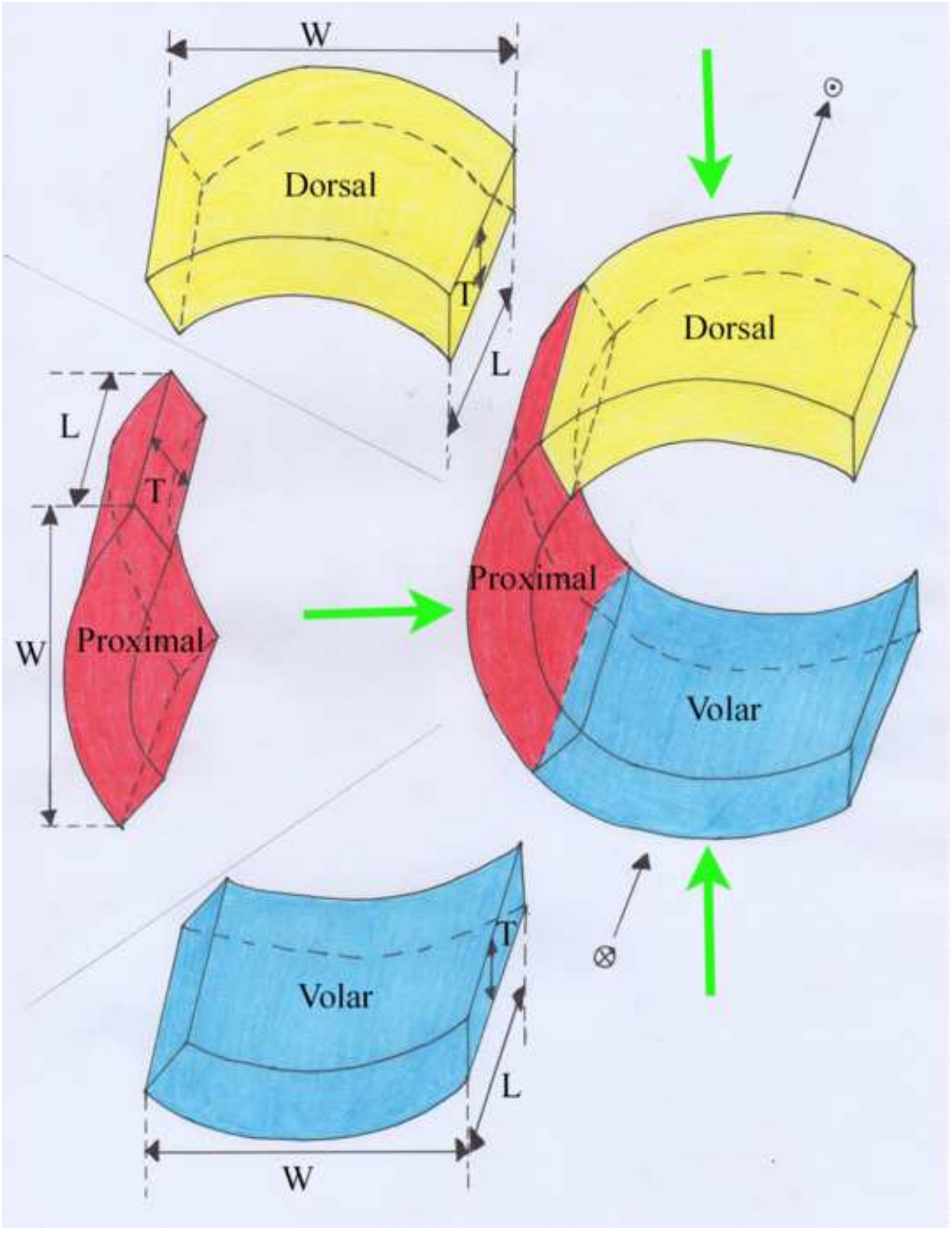

Figure 4

Click here to access/download;Figure;Figure 4 revised .tif

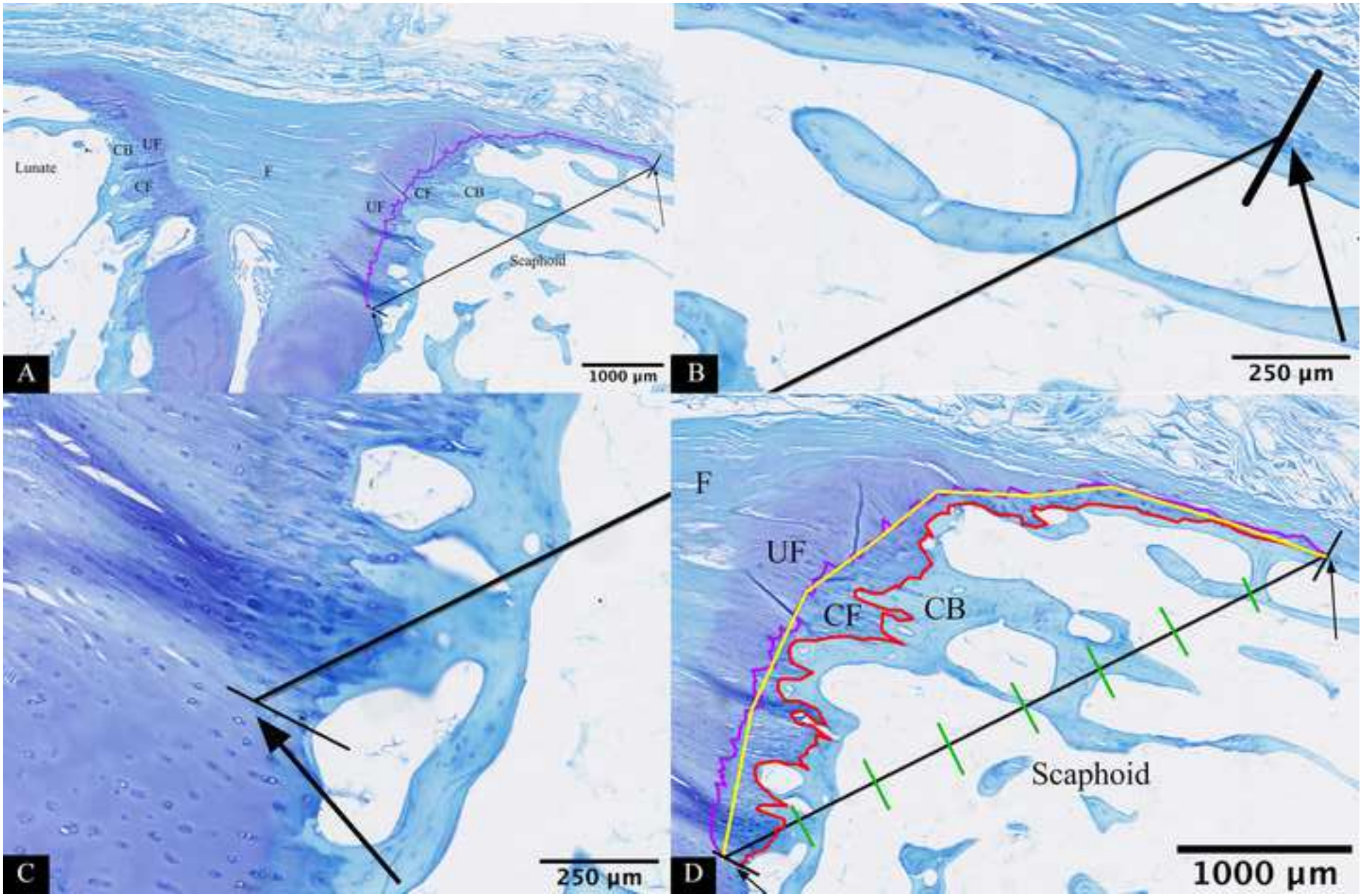

Figure 5

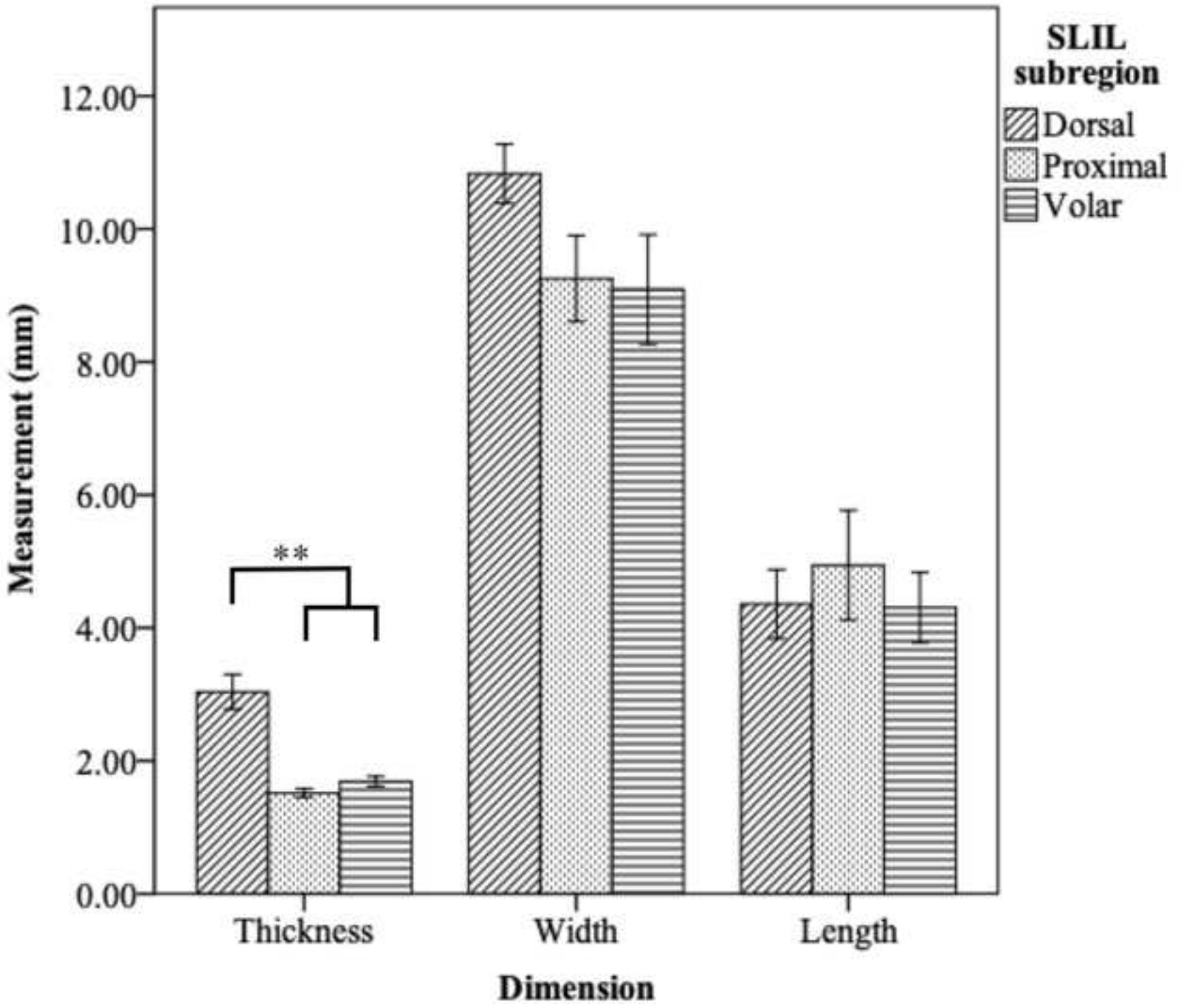

Figure 6

Click here to access/download;Figure;Figure 6.tif

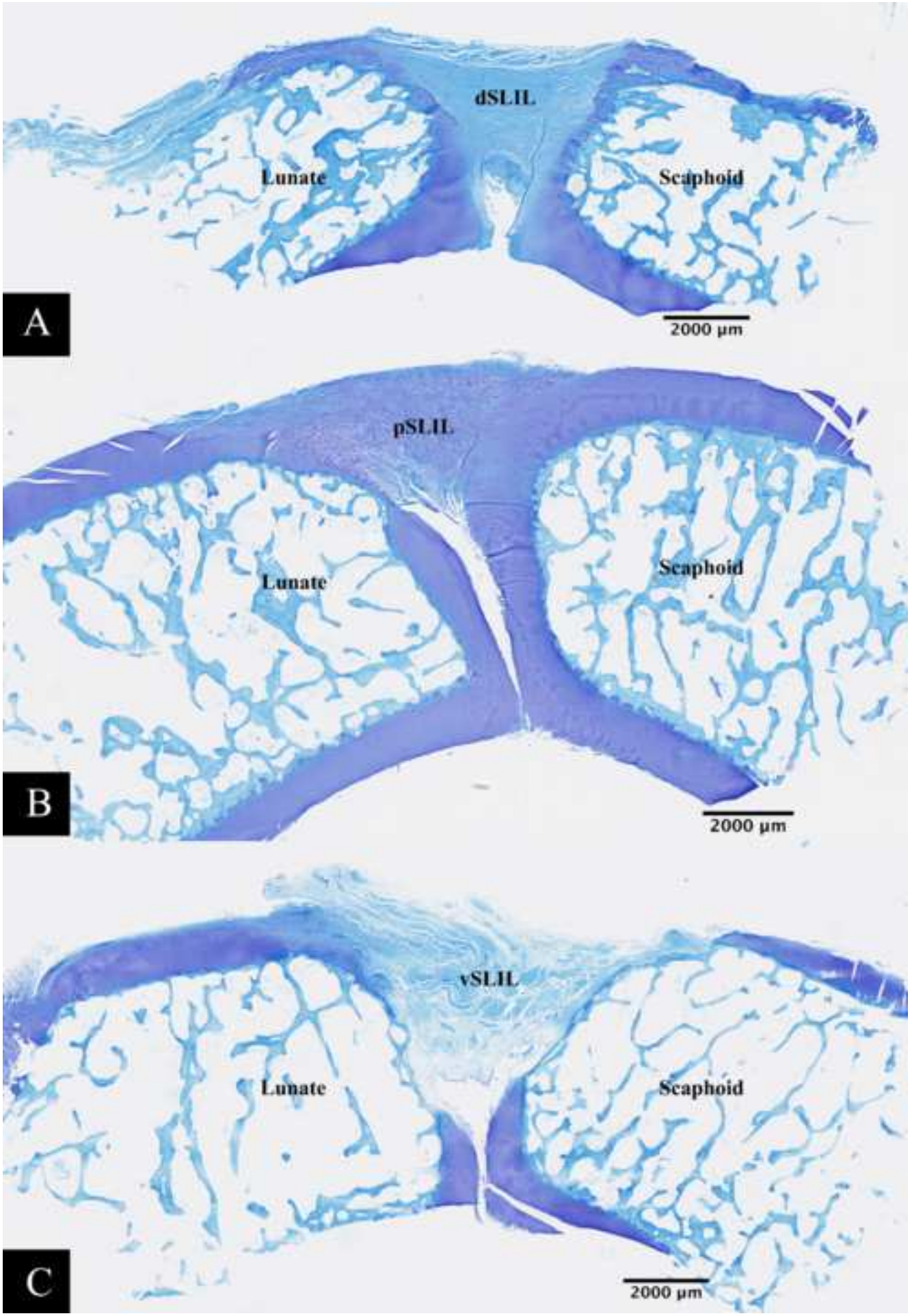

Figure 7

Click here to access/download;Figure;Figure 7.tif

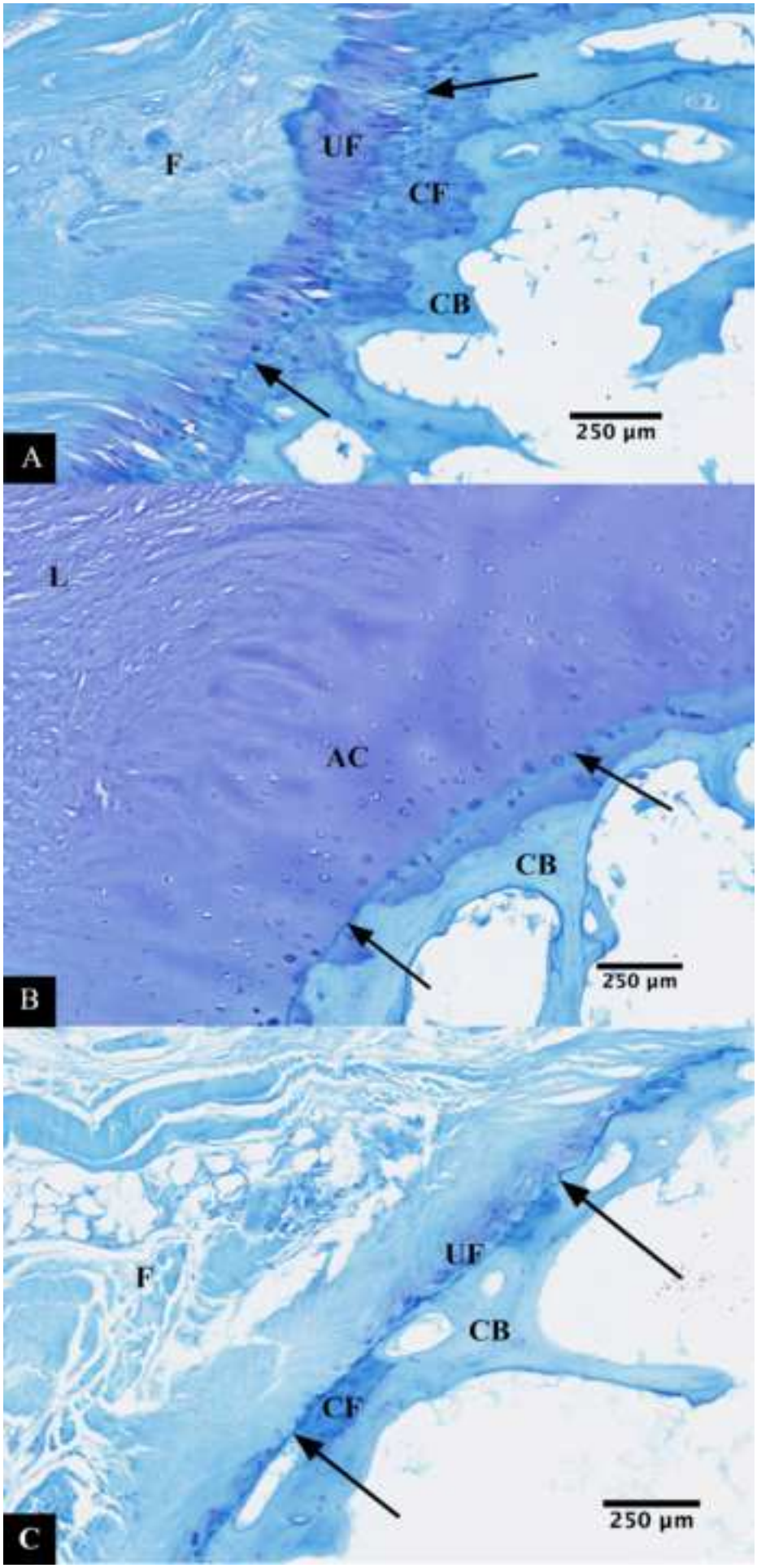

Figure 8